

1 **Assessment of the evolution of the redox conditions in a low and intermediate level**
2 **nuclear waste repository (SFR1, Sweden)**

3
4 Lara Duro^a, Cristina Domènech^{a,1}, Mireia Grivé^a, Gabriela Roman-Ross^a, Jordi Bruno^a,
5 Klas Källström^b

6
7 ^aAmphos 21 Consulting S.L. Passeig de Garcia i Fària, 49-51, 1^o-1^a - E08019 Barcelona
8 ([Spain](#)) Tel.: +34 935 830 500

9 ^bSvensk Kärnbränslehantering AB, Avd. Låg- och medelaktivt avfall, Box 250, 101 24
10 Stockholm, Sweden.

11 ¹Present address: [Grup de Mineralogia Aplicada i Medi Ambient, Dept. De](#)
12 [Cristal·lografia, Mineralogia i Dipòsits Minerals, Facultat de Geologia, Universitat de](#)
13 [Barcelona, c/Martí i Franquès s/n, 08028 Barcelona, Spain.](#) Tel.: +34 934 021 341

14
15 Corresponding author: Lara Duro; lara.duro@amphos21.com

16
17 **ABSTRACT**

18
19 The evaluation of the redox conditions in an intermediate and low level radioactive
20 waste repository such as SFR1 (Sweden) is of high relevance in the assessment of its
21 future performance.

22
23 The SFR1 repository contains heterogeneous types of wastes, of different activity levels
24 and with very different materials, both in the waste itself and as immobilisation matrices
25 and packaging. The level of complexity also applies to the different reactivity of the
26 materials, so that an assessment of the uncertainties in the study of how the redox
27 conditions would evolve must consider different processes, materials and parameters.

28
29 This paper provides an assessment of the evolution of the redox conditions in the SFR1.
30 The approach followed is based on the evaluation of the evolution of the redox
31 conditions and the reducing capacity in 15 individual waste package types, selected as
32 being representative of most of the different waste package types present or planned to
33 be deposited in the SFR1. The model considers different geochemical processes of

Formatat: Numeració: Contínua

Suprimit: SPAIN

Formatat: anglès (EUA)

Formatat: anglès (EUA)

Codi de camp canviat

35 redox relevance in the system. The assessment of the redox evolution of the different
36 vaults of the repository is obtained by combining the results of the modelled individual
37 waste package types.

38

39 According to the model results, corrosion of the steel-based material present in the
40 repository keeps the system under reducing conditions for long time periods. The
41 simulations have considered both the presence and the absence of microbial activity. In
42 the initial step after the repository closure, the microbial mediated oxidation of organic
43 matter rapidly causes the depletion of oxygen in the system. The system is afterwards
44 kept under reducing conditions, and hydrogen is generated due to the anoxic corrosion
45 of steel. The times for exhaustion of the steel contained in the vaults vary from 5 ky to
46 more than 60 ky in the different vaults, depending on the amount and the surface area of
47 steel. After the complete corrosion of steel, the system still keeps a high reducing
48 capacity, due to the magnetite formed as steel corrosion product.

49

50 The redox potential in the vaults is calculated to evolve from oxidising at very short
51 times, due the initial oxygen content, to very reducing at times shorter than 5 years after
52 repository closure. The redox potential imposed by the anoxic corrosion of steel and
53 hydrogen production is on the order of -0.75 V at pH 12.5. In case of assuming that the
54 system responds to the Fe(III)/Magnetite system, and considering the uncertainty in the
55 pH due to the degradation of the concrete barriers, the redox potential would be in the
56 range -0.7 to -0.01V.

57

58 A Monte-Carlo probabilistic analysis on the rate of corrosion of steel shows that the
59 reducing capacity of the system provided by magnetite is not exhausted at the end of the
60 assessment period, even assuming the highest corrosion rates for steel.

61

62 Simulations assuming presence of oxic water due to glacial melting, intruding the
63 system 60 ky after repository closure, indicate that magnetite is progressively oxidised,
64 forming Fe(III) oxides. The time at which magnetite is completely oxidised varies
65 depending on the amount of steel initially present in the waste package.

66

67 The behaviour of Np, Pu, Tc and Se under the conditions foreseen for this repository is
68 discussed.

Suprimit: ,000

Suprimit: years

Suprimit: ,000 years

Suprimit: ,000

Suprimit: years

74

75 **KEYWORDS**

76

77 Redox evolution

78 Nuclear waste repository

79 Radionuclide migration

80 Reductive capacity

81

82 **1. INTRODUCTION**

83

84 Redox conditions of a nuclear waste repository are of high relevance in the assessment
85 of the future behaviour of the repository and the deposited wastes. The study of the
86 evolution of the redox conditions presents a high level of complexity due, among other
87 reasons, to the variety of the materials that can be present in the facility and react
88 simultaneously. The assessment of redox conditions can only be approximated by
89 adequately discussed assumptions (Wanner, 2007). Uncertainties concerning processes,
90 parameters and materials must be also assessed and evaluated.

91 The most usual way to define the redox state of a system is based on the measure or
92 determination of the redox potential (Eh), which can be related to the concentration of
93 the redox active species in the system. Nevertheless, redox reactions are known to be
94 slow and in many cases they need the action of catalysts to proceed, despite being
95 thermodynamically favoured. Thermodynamic equilibrium among redox species can not
96 be granted and this precludes the achievement of conclusions on the redox state of a
97 system simply based on the determination of redox active species.

98

99 This implies that the simple monitoring and calculation of redox potentials is sometimes
100 not a very good indicator of the redox state of all redox couples in the system, as it has
101 been proven from many groundwater analyses that different redox potentials can be
102 measured depending on the redox couple considered to be in equilibrium in the system
103 (Lindberg and Runnells, 1984).

104

105 The redox potential is identified as one of the main chemical parameters affecting the
106 chemical behaviour of radionuclides and consequently their mobility. The study of the

107 redox conditions of repositories requires an understanding on the processes affecting the
108 existing materials and the rates at which the processes occur under the different
109 conditions expected to prevail in the system.

Suprimir: in this type

110
111 Different attempts, normally site-specific studies, have been undertaken to determine
112 the future evolution of the redox conditions in a low and intermediate level nuclear
113 waste repository (Neall, 1994; Humpreys et al., 1997; Small et al., 2000&2008; Wersin
114 et al., 2003; Grivé et al., 2011; Avis et al., 2012).

115
116 The objective of the work summarised here is to develop a methodology to calculate the
117 evolution of the redox state of the SFR1 repository with deposition time. According to
118 the Swedish regulations, the time frame for the assessment as must span over the
119 maximum risk consequences with a maximum of 100 ky after repository closure (SSM,
120 2008). The model should be transferrable to a new configuration of the repository,
121 possible extension, or changes in the type and/or composition of the waste packages
122 deposited.

Suprimir: ,000 years

Suprimir: Reference to SSMFS 2008:37

123
124 To this aim, a geochemical model has been developed that accounts for the inventory of
125 the SFR1 facility and considers the most up to date scientific understanding of the redox
126 and chemical processes likely to drive the redox evolution of the system. The model has
127 been developed by individual waste packages and deposition vaults and has been
128 applied to obtain the redox evolution of the complete repository system.

129
130 Due to the huge amounts of materials present in the system, such as metals and organic
131 matter, in comparison with the amounts of redox sensitive radionuclides, it is very
132 unlikely that the radionuclides can have any relevant effect on the redox evolution of the
133 system. Nevertheless, the implications that chemical changes can have on the behaviour
134 of redox sensitive nuclides, Np, Pu, Tc and Se, under the conditions developed in the
135 repository are presented.

S'ha desplaçat (inserció) [1]

136
137 1.1. The system under study: the SFR1 Repository

Suprimir: ¶

Suprimir: REPOSITORY

138

144 The SFR1 repository at Forsmark in Sweden is used for the final disposal of low- and
145 intermediate-level radioactive waste (L/ILW) produced by the Swedish nuclear power
146 program, industry, medicine and research. Waste disposed in SFR1 belongs to the short-
147 lived waste category according to the IAEA definition (IAEA, 2009). This means that
148 there is a limitation of long-lived α -activity of an average overall of 400 Bq/g per waste
149 package, allowing a maximum per individual waste package of 4,000 Bq/g.

150
151 The repository system is placed in a shallow subsurface area of Forsmark under the
152 Baltic Sea. It consists of four different vaults: the Silo and the BMA, BLA and 1&2BTF
153 vaults. More details can be found in SKB (2008) and will not be repeated here. [A sketch](#)
154 [of the system showing the different vaults is shown in Figure 1.](#)

155
156 The SFR1 system presents a high capacity to buffer an oxidant intrusion, given the
157 amount of materials prone to oxidise. The most relevant characteristics of the repository
158 for the purpose of the redox assessment presented here are that (1) the wastes are
159 predominantly conditioned in concrete matrices; (2) bitumen is also used as matrix for
160 some wastes; (3) the waste packages are made of concrete or steel, and (4) the wastes,
161 although very varied in composition, contain important amounts of metals and organic
162 materials, including cellulose.

163
164 About fifty different type of waste categories are foreseen to be deposited in the SFR1
165 until its closure (approx. at year 2050). They can be represented by 15 generic waste
166 packages (see [Table 1](#)) differing in the type and materials of the container, type and
167 amount of immobilising matrix and type and amount of waste.

168
169 The amount of the different materials to be deposited in each one of the vaults of the
170 SFR1 repository at the time of its closure (at year 2050) is shown in [Figure 2](#) (data from
171 Almkvist and Gordon, 2007).

172
173 In the light of the amount of materials present in the repository, many redox processes
174 can be identified as being of relevance in the SFR system: metal corrosion, degradation
175 of organic matter, radiolysis, sulphate reduction, gas generation and fermentation,...
176 The level of radiation that may cause generation of oxidants in the repository is very
177 low and previous assessments on the influence that radiolysis can have on the oxidant

Suprimit:

Suprimit: Table 1

Suprimit: Figure 1

181 balance of the repository, such as the one in Moreno et al. (2001) have shown that this
182 effect is expected to be minimal.

183

184

185

186

187

189

190 Therefore, processes that a priori can have a larger influence in the short and long-term
191 redox evolution of the repository are:

- 192 • Metal corrosion
- 193 • Organic matter degradation (bitumen, non-classified organic matter and
194 cellulose)
- 195 • Microbial activity

196

197 An important feature of the repository is the ubiquity of concrete and cement, what
198 conditions the system to high pH values.

199

200 Just after repository closure, there will be oxidants in the system due to repository
201 construction and operation periods, and under non-disturbed conditions it is foreseen
202 that these oxidants will be rapidly consumed and the system will reach anoxia and later
203 develop reducing conditions. Groundwaters reaching the repository at long-term are not
204 expected to contain appreciable concentrations of oxidising species, due to their prior
205 interaction with soils and minerals that will cause oxidant consumption. According to
206 the expected evolution of the SFR1 environment (SKB, 2008), the only possibility of
207 oxidising conditions to reach repository depths arises from an inflow of glacial oxygen-
208 rich and diluted water. This situation would, if at all, happen during ice melting events.
209 According to the foreseen climatic evolution of the system, the earliest time at which
210 melting water would reach the repository is 60 ky after its closure. This means that,
211 once the system has reached reducing conditions, its capability to buffer an oxidising
212 intrusion will basically remain the same until 60 ky and that after this time, it will be
213 jeopardised only in the case of melting ice water inflowing the system.

214

Suprimir: Table 1. Representative waste packages in each one of the vaults of the SFR1 repository (SILO, BMA, 1 and 2 BTF and BLA), amounts of the different materials contained and porosity of the wastes. Data from Almkvist and Gordon (2007) and updated inventory. Φ: porosity; BIT: bitumen; GOM: non classified organic matter. CELL: cellulose.¶

Formatat: anglès (EUA)

Formatat: anglès (EUA)

Formatat: anglès (EUA)

Formatat: anglès (EUA)

Taula formatada

Formatat: anglès (EUA)

Formatat: anglès (EUA)

Formatat: anglès (EUA)

Formatat: anglès (EUA)

Formatat: anglès (EUA)

Formatat: anglès (EUA)

Formatat: anglès (EUA)

Taula formatada

Formatat: anglès (EUA)

Formatat: anglès (EUA)

Formatat: anglès (EUA)

Formatat: anglès (EUA)

Formatat: anglès (EUA)

Formatat: anglès (EUA)

Formatat: anglès (EUA)

Formatat: anglès (EUA)

Formatat: anglès (EUA)

Formatat: anglès (EUA)

Formatat: anglès (EUA)

Formatat: Tipus de lletra: (Per defecte) Times New Roman, 12 pt

Formatat: anglès (EUA)

Formatat: anglès (EUA)

Formatat: anglès (EUA)

Formatat: anglès (EUA)

Suprimir: .000

Suprimir: years

Suprimir: .000 years

224 Metallic corrosion and organic matter degradation (either biotically-mediated or
 225 chemical) will provide most of the capacity of the system to buffer any potential oxidant
 226 intrusion. However, although the reducing capacity of the repository can be far larger
 227 than the one needed to account for total consumption of the oxygen initially trapped, the
 228 kinetics of the electron-transfer processes must be considered to assess the redox
 229 evolution of the system with time.

230
 231 A qualitative sketch of the expected evolution of the redox conditions in the repository
 232 is shown in [Figure 3](#). The sketch shows the time scale, the different redox processes
 233 occurring, microbes involved, and a redox scale in the right, with the different redox
 234 potential achieved in the system if equilibrium with the main redox pairs is calculated at
 235 pH = 12.5, which corresponds to equilibrium with portlandite, Ca(OH)₂(s), as a proxy
 236 for concrete.

237

238

239 2. MODELLING METHODOLOGY

240

241 When assessing the behaviour of this type of systems it is important to consider not only
 242 the theoretical capacity that the system has to accept oxidants (ReDucing Capacity or
 243 RDC, Scott and Morgan (1990)), but also the relative rate of reduction versus the rate at
 244 which the oxidant intrusion occurs. Therefore, the conceptual and numerical models
 245 developed include:

246

247 -the assessment of the time evolution of the system, i.e., the rate at which reducing
 248 conditions are attained and how fast it reacts towards an oxidant intrusion; and,

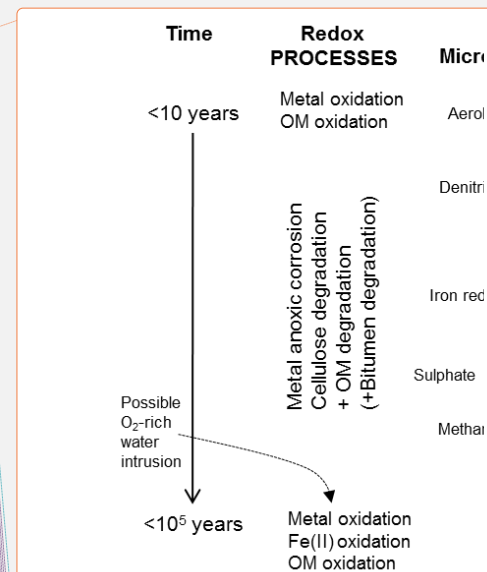
249 -the assessment of the remaining buffer capacity of the system in the case of any future
 250 oxidising disturbance, that is, the RDC.

251

252 The different vaults of the repository have been considered as a combination of generic
 253 waste package types. In this way, the combination of the evolution of the redox
 254 conditions in each generic waste package type is used to assess the evolution of the
 255 redox conditions in the vaults and this, in turn, in the complete repository system.

256

Suprimit: Figure 2



Suprimit:
 Figure 2. Sketch showing the evolution of the redox potential in SFR1 under non disturbed conditions, depending on the redox couple governing the Eh, at a pH 12.5 (portlandite equilibrium).¶

Formatat: Tipus de lletra: (Per defecte) Times New Roman, 12 pt

Formatat: anglès (EUA)

Formatat: anglès (EUA)

Formatat: anglès (EUA)

Formatat: anglès (EUA)

Suprimit: ising

263 The following approach has been implemented in the model.

264

265 a. Calculation of the chemical evolution of each one of the 15 different types of
266 waste packages presented in [Table 1](#), by implementing the relevant redox processes into
267 a conceptual and numerical model.

Suprimit: Table 1

268 b. From the results in a., calculation of the temporal evolution of the RDC of each
269 one of the 15 types of waste packages.

270 c. Combination of the results from b. to obtain the RDC at each time for each one
271 of the vaults Silo, BMA, BLA and [1&2BTF](#).

Suprimit: 1BTF, 2BTF

272 d. Combination of the results from c. to calculate the RDC of the complete SFR1.

273

274 With the aim of monitoring the role of the different processes responsible for the redox
275 evolution of the system, three temporal scales have been implemented in the model: a
276 very short term (up to 30 days), short term (up to 5 years) and long term (from 5 years
277 to 100 [ky](#)).

Suprimit: ,000

Suprimit:

Suprimit: ears

S'ha desplaçat cap amunt [1]: Due to the huge amounts of materials such as metals and organic matter, in comparison with the amounts of redox sensitive radionuclides, it is very unlikely that the radionuclides can have any relevant effect on the redox evolution of the system. Nevertheless, the implications that chemical changes can have on the behaviour of redox sensitive nuclides, Np, Pu, Tc and Se, under the conditions developed in the repository are presented. ¶

278

279

280

281 3. CONCEPTUAL AND NUMERICAL MODEL

282

283 The rate and extent of the different redox processes occurring in the system is discussed
284 in the light of the available data in the literature. Several assumptions are made for the
285 sake of the modelling procedure, as presented below.

286

287 3.1. Redox processes and implementation

288

289 3.1.1. Metal corrosion

290

291 In the presence of oxygen, iron corrosion produces Fe(III) oxides and hydroxides.

292 Hematite is the thermodynamically stable Fe(III) oxide in the stability field of water

293 followed by goethite and ferrihydrite or hydrous ferric oxides. However, despite their

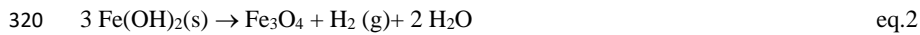
294 lower stability with respect to hematite, goethite and hydrous ferric oxides can prevail

307 as metastable solid phases for long time periods and they have faster formation kinetics
308 when metallic iron oxidises in the presence of oxygen than hematite.

309

310 In the absence of oxygen, iron can corrode through water reduction given that Fe(s) is
311 thermodynamically unstable in water. As for the corrosion of other metals also present
312 in the system, such as aluminium and zinc, H₂(g) is generated (eq.1). Fe(OH)₂(s) is
313 metastable and with time evolves towards magnetite, according to the Schikorr reaction
314 (eq.2). The composition of the magnetite formed on the surface of iron is not exactly
315 known, although it has been suggested that it consists of an oxide Fe_{3-x}O₄ with a spinel-
316 like structure varying in composition from Fe₃O₄ (magnetite), in oxygen-free solutions,
317 to Fe_{2.67}O₄ under the presence of oxygen (Stumm and Morgan, 1996).

318



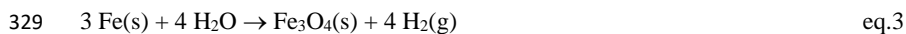
321

322 In the presence of carbonate, sulphide or chloride, iron corrosion can lead to the
323 formation of other corrosion products different from magnetite, such as iron sulphides,
324 carbonates or green rusts.

325

326 Eq.3 shows the global redox reaction for the transformation of iron into magnetite under
327 anoxic conditions.

328



330

331 Iron corrosion under both oxic and anoxic conditions is a process kinetically controlled.
332 Corrosion rates are influenced by different parameters such as composition of the
333 material, temperature, groundwater composition, presence and composition of gases,
334 evolution of the surface (whether it has been previously corroded or not), etc. Corrosion
335 products may form a protective layer on the steel surface, and cause a decrease of the
336 corrosion rate with time, as observed from experimental data (Smart et al. 2010 and
337 references therein). Steel corrosion rates used in this work are presented in [Table 2](#) and
338 have been selected after an extensive literature review.

339

Suprimit: Fe(s)

Suprimit: Table 2

342 It is relevant to point out that fast corrosion of Al and Zn has been pessimistically
343 neglected in the model approach. These metals are present only in very specific
344 locations, not in all the waste packages, as Fe-bearing metals, and are therefore not
345 considered to provide an important reducing capacity to the system in comparison with
346 iron and steel.

Formatat: Tipus de lletra: 12 pt, Color de la lletra: Automàtic, anglès (Regne Unit)

Formatat: Esquerra

Formatat: Tipus de lletra: 12 pt, Color de la lletra: Automàtic, anglès (Regne Unit)

Formatat: Tipus de lletra: 12 pt, Color de la lletra: Automàtic, anglès (Regne Unit)

Formatat: Tipus de lletra: 12 pt, Color de la lletra: Automàtic, anglès (Regne Unit)

Formatat: Tipus de lletra: 12 pt, Color de la lletra: Automàtic, anglès (Regne Unit)

Formatat: Tipus de lletra: 12 pt, Color de la lletra: Automàtic, anglès (Regne Unit)

Formatat: Tipus de lletra: 12 pt, Color de la lletra: Automàtic, anglès (Regne Unit)

Formatat: Tipus de lletra: 12 pt, Color de la lletra: Automàtic, anglès (Regne Unit)

Formatat: Color de la lletra: Automàtic

Formatat: Tipus de lletra: No Negreta, No Cursiva, Color de la lletra: Automàtic

347
348 3.1.2. Degradation of Organic Matter: bitumen, generic organic matter and cellulose.

349

350 Under highly alkaline conditions, bitumen can be subjected to microbially-mediated
351 degradation (Zobell and Molecke, 1978; Roffey and Norqvist, 1991).

352

353 Biodegradation of bitumen is a complex process given that each of its components can
354 degrade at different rates (Petersson and Elert, 2001; Pedersen, 2001). There is
355 increasing evidence for the generation of soluble organic compounds from natural
356 organic matter under hyperalkaline conditions (Claret et al., 2003; Elie et al., 2004). The
357 constituents of the industrial bitumen such as that used in SFR1 repository (Petersson
358 and Elert, 2001) are the same than those identified in natural bitumen and petroleum
359 although they may differ in their proportions (Faure et al., 1999).

360

361 The conceptual model assumes that generic organic matter and bitumen are degraded
362 under alkaline and near neutral conditions. Degradation is microbially mediated under
363 biotic conditions and organic matter and bitumen are chemically degraded once abiotic
364 conditions are achieved. Acetate is assumed as the main representative product of both
365 microbial and chemical degradation.

366

367 Bitumen has been represented by the stoichiometry $C_{7.33}H_{10.91}O_{0.06}$ (Petersson and Elert,
368 2001) while the non-classified or generic organic matter reported in the waste packages
369 has been attributed a generic composition of CH_2O . The same mechanism is considered
370 for both “generic organic matter” and bitumen degradation (eq.4).

Suprimit: model

371

372 $C_{7.33}H_{10.91}O_{0.06} + 7.28 H_2O \rightarrow 3.67 CH_3COO^- + 10.8 e^- + 14.47 H^+$ eq.4

373

374 The three different generic microbial communities considered to be present in the
375 repository (O_2 - consumers (aerobes); iron reducing bacteria (IRB) and sulphate reducing

Suprimit: iron reduction bacteria

378 bacteria (SRB)) contribute to the degradation of bitumen, generic organic matter,
379 acetate and/or cellulose and also depend on these substrates to survive.

380

381 The biological activity of each microbial group is modelled according to the extended
382 Monod growth model (Rittmann and Van Briesen, 1996; Sena, 2009) as shown in [Table](#)
383 [2](#). Electron acceptors in the process are oxygen, ferric iron and sulphate. In order to
384 implement the bacterial activity and growth in the system, a threshold concentration of
385 10^{-6} M for each one of these three electron acceptors has been defined, so that inactivity
386 of aerobes is considered for oxygen concentrations below 10^{-6} M, inactivity of IRB is
387 assumed for ferric iron concentrations below 10^{-6} M and inactivity of SRB for sulphate
388 content below 10^{-6} M. These thresholds are in the order of values reported in the
389 literature (McMahon and Chapelle, 2008; Small et al., 2008; Appelo and Postma, 2005;
390 and references therein).

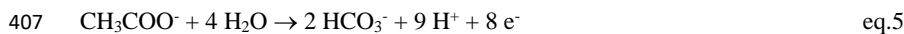
391

392 Under abiotic conditions, that is, when electron acceptor concentrations are too low to
393 keep microbes active, generic organic matter and bitumen are assumed to chemically
394 degrade at a constant rate, equal to 10^{-12} mol dm⁻³ s⁻¹, two orders of magnitude below
395 the biotic rate. [Table 2 and Table 3](#) show the values of the parameters for these
396 equations.

397

398 In the model it is assumed that acetate generated during organic matter degradation
399 microbially degrades to carbonate according to eq.5. As in the case of bitumen and
400 generic organic matter, the acetate biotic degradation rate is controlled by the growth
401 rate of aerobes, IRB and SRB and the availability of O₂, Fe(III) or S(VI) in solution.
402 In agreement with the available information in the literature, it is assumed that acetate
403 cannot further degrade abiotically. Thus, once abiotic conditions are achieved, acetate
404 accumulates in solution and can precipitate in the form of Ca(CH₃COO)₂ (s) if
405 oversaturated.

406



408

409 Degrading cellulose is considered from a monomer of cellulose already hydrolysed
410 (C₆H₁₂O₆ in eq.6).

Suprimit: ,

Suprimit: Table 2.

Suprimit: Table 2 and Table 3

Suprimit:

415

416 Under oxic conditions, ($[O_2] > 10^{-6} \text{ mol dm}^{-3}$), these previously hydrolysed cellulose
417 monomers degrade to carbonate, although this reaction is often not complete leading to
418 acetate and carbon dioxide, according to eq.7.

Suprimit: ate

419

420 Under anoxic conditions, approximately 80% of the products generated in the
421 degradation process of cellulose are isosaccharinic acid compounds (ISA) (Van Loon
422 and Glaus, 1994). For the sake of simplicity, eq.8 is used for cellulose degradation under
423 alkaline anoxic conditions and has been defined after assuming that 80% of cellulose
424 degrades to ISA and 20% to acetate.

Suprimit: g

Suprimit: (

425

426 Given the high aqueous concentration of Ca under cementitious conditions and the
427 increase of aqueous concentration of ISA foreseen because of cellulose degradation,
428 $\text{Ca}(\text{HISA})_2$ (cr) can precipitate if oversaturated.

429

430 As in the case of bitumen and acetate, cellulose degradation under biotic conditions is
431 controlled by the growth of O_2^- , Fe(III)- and S(VI)-reducing bacteria and the availability
432 of O_2 , Fe(III) or S(VI) in solution.

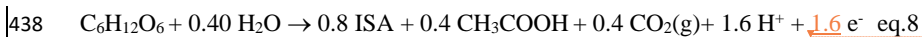
433



435



437



Suprimit: 3.2

439

440 Glaus et al. (1999), Van Loon et al. (1999) and Glaus and Van Loon (2008) studied the
441 abiotic degradation of cellulose under alkaline conditions and proposed that the peeling-
442 off reaction is responsible for an initial fast reaction phase (between 2 and 3 years
443 depending on the cellulose type), while a later slower phase depends on the amount of
444 cellulose available for reaction (Glaus and Van Loon, 2008, Knill and Kennedy, 2003).

445

446 Based on the results of their experiment, Glaus and Van Loon (2008) proposed the
447 kinetic law shown in eq.9, where celdeg is the fraction of cellulose degraded as a

452 function of time, k_i different reaction constants and G_i the reciprocal of the starting
453 degree of polymerization. This rate has been used in the present model.

454

455
$$celdeg_{cellulose} = 1 + e^{-k_h t} \left[\frac{k_1}{k_2} (G_i)_o (1 - e^{-k_h t}) - 1 \right]$$
 eq.9

458

459

460

461

462

463 3.2. Flow, boundary and initial conditions

464

465 During the operational period, the repository is open to air, thus it is not water saturated.

466 This study has been done assuming that the re-saturation is very fast after repository

467 closure. According to Holmen and Stigsson (2001) the time needed for complete

468 saturation of the repository is very short in comparison with the 100 ky considered in

469 this study. It has been also considered that water is always available and accessible for

470 chemical reactions.

471

472 Gases generated from corrosion of steel and chemical or microbial degradation of

473 cellulose, bitumen and other organic materials such as H_2 , CH_4 and $CO_2(g)$ in case of

474 non-alkaline conditions can dissolve in the contacting water. Gases will be able to form

475 an individual gas phase and leave the system only in case an overpressure is created.

476 The hydrostatic pressure at 70 m depth is 6.87 atm.

477

478 The numerical model neither considers the transport or diffusion of gases through the

479 container wall nor the mechanical effects on the system that the presence of these gases

480 can produce.

481

482 Initial porewater of the different waste package types is considered to be in equilibrium

483 with atmospheric O_2 , at P_{O_2} of 0.21 atm, due to the construction and operational

484 periods; and in equilibrium with portlandite in those cases where concrete has been used

485 as waste matrix and/or groundwater has interacting with the repository structures (made

486 of concrete) before reaching the waste. This occurs in all cases except for waste package

Formatat

Suprimir: Table 2. Kinetic rRates used in the calculations. Rates in mol dm⁻³ s⁻¹, except when indicated. Values for parameters listed in Table 3.¶

Steel corrosion rate

Formatat: anglès (EUA)

Formatat

Formatat

Formatat: anglès (EUA)

Formatat: anglès (EUA)

Formatat: anglès (EUA)

Formatat: anglès (EUA)

Formatat: anglès (EUA)

Formatat: anglès (EUA)

Formatat: anglès (EUA)

Formatat: anglès (EUA)

Formatat: anglès (EUA)

Formatat: anglès (EUA)

Formatat: anglès (EUA)

Formatat: anglès (EUA)

Formatat: anglès (EUA)

Formatat: anglès (EUA)

Formatat: anglès (EUA)

Formatat

Formatat: anglès (EUA)

Formatat: anglès (EUA)

Formatat: anglès (EUA)

Formatat: anglès (EUA)

Formatat: anglès (EUA)

Formatat: anglès (EUA)

Formatat: anglès (EUA)

Formatat: anglès (EUA)

Formatat: anglès (EUA)

Formatat

Formatat: Espanyol (Espanya)

Formatat

Suprimir: by assuming that the re-saturation is very fast after

Suprimir: of

501 O.12, for which initial waste porewater is considered to be a granitic porewater.

502 Groundwater compositions are listed in [Table 4](#).

503

504 [The studied radionuclides are Se, Tc, Np and Pu which, besides U, are the main redox](#)
505 [sensitive radionuclides present in SFR1. The analysis presented here has been](#)
506 [conducted by assuming that the initial concentration of the radionuclides in the system](#)
507 [is given by the dissolution of the complete inventory in the total void volume of the](#)
508 [vaults \(void volume is completely water saturated\) \(Figure 4\).](#)

509

511 [3.3. Code and Thermodynamic Data Base](#)

512

513 The model has been run with the code PHREEQC (Parkhurst and Appelo, 1999) and the
514 thermodynamic database SKB_TDB_2009. [This thermodynamic database is based on](#)
515 [the selection by Hummel et al. \(2002\) with modifications reported in Duro et al. \(2006,](#)
516 [2010, 2012\) for the sulphur, iron and carbonate systems”](#)

517

518 [3.4. Calculation of the Reducing capacity \(RDC\) of the system](#)

519

520 Scott and Morgan (1990) proposed the concepts of [OXidising](#) and ReDucing Capacities
521 (OXC and RDC) in analogy to [quantities](#) such as total acidity or alkalinity in the case of
522 acid/base systems. They defined the reductive capacity as the sum of all reductants that
523 can be oxidised by strong oxidants (e.g., O₂) to a preselected equivalence point, which is
524 the Electron Reference Level (ERL). The RDC of a system gives, thereof, an estimation
525 of its capacity to accept oxidants, i.e., is a chemical sum of the maximum amount of
526 oxidants that the system is able to buffer.

527

528 The generic definition of RDC is shown in eq.10, where [Red] and [Ox] are,
529 respectively, the concentration of reducing and oxidising species present in the system,
530 and n_i and n_j are the number of electrons involved in the redox reactions.

531

$$532 \text{RDC} = \sum_i n_i \times [\text{Red}] - \sum_j n_j \times [\text{Ox}] \quad \text{eq.10}$$

533

Suprimir: Table 4.

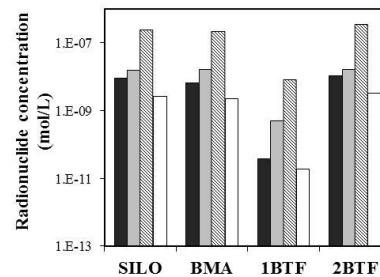
Suprimir: Table 4. Composition of the cementitious and granitic porewater used in the calculations. From SKB (2008). &From Salas et al. (2010).¶

Formatat: Tipus de lletra: 12 pt

Suprimir: ¶

Formatat: Tipus de lletra: 12 pt

Suprimir: (Figure 3



Suprimir: Figure 3. Calculated concentrations of Np, Pu, Tc and Se resulting from dissolving the complete inventory in the saturated void volume. ¶

Formatat: anglès (EUA)

Formatat: anglès (EUA)

Formatat: anglès (EUA)

Formatat: anglès (EUA)

Suprimir: ¶

Suprimir: 2

Suprimir: . This database is the database of Hummel et al. (2002) with some modifications reported in Duro et al. (2006), and included in the thermodynamic database ThermoChimie (Duro et al. 2010, 2012) issued together with PHREEQC code for the S, Fe, C aqueous species and solid phases.¶

Suprimir: 3

Suprimir: OxiDising

Suprimir: magnitudes

554 Given the relevance that the iron system has in this environment, we have defined as
555 electron reference level the most oxidised form of iron, Fe(III). By considering this,
556 eq.11 and eq.12 are used to calculate both terms of eq.10.

557

$$\sum n_i \times [\text{Red}] = [\text{Fe}(0)] \times 2 + [\text{Fe(II)(aq)}] \times 1 + [\text{magnetite}] \times 1 + [\text{HS}^-] \times 8 + [\text{bitumen}] \times 11 + [\text{organic matter}] \times 11 + [\text{cellulose}] \times 3.2 + [\text{acetate}] \times 8 + [\text{H}_2] \times 2 \quad \text{eq.11}$$

560

$$\sum n_i \times [\text{Ox}] = [\text{O}_2] \times 4 \quad \text{eq.12}$$

562 Given the uncertainty existing on the reactivity of H₂(g) and on the role of bitumen as
563 reducing agent fast enough to occur in the timeframe and under the conditions of the
564 assessment, the contribution of H₂(g) to the RDC of the system has not been included in
565 the calculation of RDC and in some cases the RDC has been calculated with and
566 without considering bitumen in the formulae.

567

568 4. RESULTS AND DISCUSSION

569

570 According to the redox processes considered in the model, different groups of waste
571 package types can be identified:

- 572 - waste package types in which only steel corrosion is considered (R.16, R.15 and
573 S.13);
- 574 - waste packages where both corrosion of steel and degradation of generic organic
575 matter are considered (O.02, R.01 and B.07/O.07);
- 576 - waste package types where both corrosion of steel and degradation of bitumen
577 are considered (B.06, F.18, F.05 and F.17);
- 578 - waste package types where besides the previous processes, cellulose degradation
579 has also been included (O.23, F.23, B.05 and O.12).

580

581 Initial concentrations differ among the waste packages types as shown in .
582 In all package types except O.12 in vault BLA pH is buffered to 12.5 due to the
583 equilibrium with portlandite, which also controls Ca²⁺ aqueous concentration.

584

585 A comparison of the time evolution towards reducing conditions depending on the
586 different redox processes considered is shown in Figure 5. As can be seen, low redox

Suprimit: _

Codi de camp canviat

Suprimit:

Suprimit: Figure 4

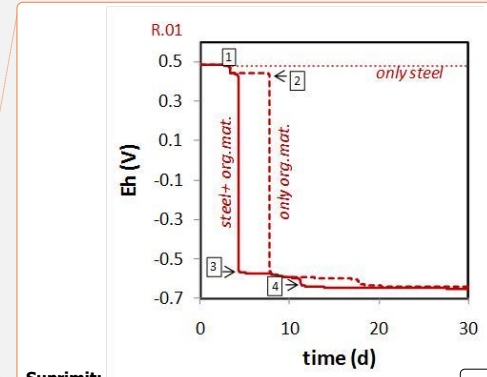
590 potentials are reached much faster when considering the processes of degradation of
 591 organic matter than when only steel accounts for oxidant consumption. This is a
 592 consequence of the different kinetics of the reactions responsible for oxidant depletion.
 593 In all those waste package types containing organic matter, the oxic period is very short
 594 (about 3.3 days). In its absence, the period exceeds 30 days, because O₂ consumption by
 595 steel corrosion is slower. In the case of O.12, where neutral pH conditions prevail, the
 596 higher steel corrosion rates shorten the oxic period to less than one day.

597
 598 **Figure 6** shows the evolution of the redox potential in a waste package in which steel
 599 corrosion is responsible for oxidant depletion. Three different stages can be appreciated:
 600 oxygen consumption, sulphate consumption and anoxic corrosion of steel. Initially, the
 601 corrosion of steel under oxidising conditions generates goethite. Further steel corrosion
 602 causes goethite consumption and formation of magnetite and hydrogen.

603
 604 The time at which all the steel initially present in the waste package is corroded depends
 605 mainly on two factors: the initial amount of steel and its reactive area. **Figure 7** shows
 606 the time period needed to corrode all the steel present in the packages. In two of the
 607 modeled cases steel is not predicted to corrode completely, even after the 100 **ky** of the
 608 assessment. That implies that the RDC of the system provided by steel will remain for
 609 long periods of time.

610
 611 The degradation of organic matter in the system has several consequences of interest for
 612 the assessment, such as the production of organic compounds that may have
 613 implications in the behaviour of radionuclides due to their ability to form complexes.
 614 Once O₂ concentration is depleted, the degradation of generic organic matter, bitumen
 615 and acetate occurs mediated by SO₄²⁻ reducing bacteria (SRB). The biotic period is
 616 considered to finish when sulphate concentration falls below 10⁻⁶M. Once SRB are no
 617 longer active, the degradation of generic organic matter or bitumen to acetate occurs
 618 following an abiotic rate, which is considered constant with time ().

619
 620 In the absence of microorganisms, acetate is not allowed to degrade to CO₂ in the
 621 model, thus accumulates in solution. The same applies to ISA produced by the
 622 degradation of cellulose under abiotic conditions. The consequence is that acetate and

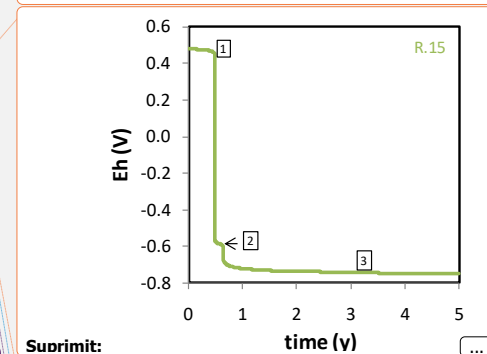


Suprimir: [icon]

Formatat: anglès (EUA)

Formatat [icon]

Suprimir: Figure 5



Suprimir: [icon]

Taula formatada

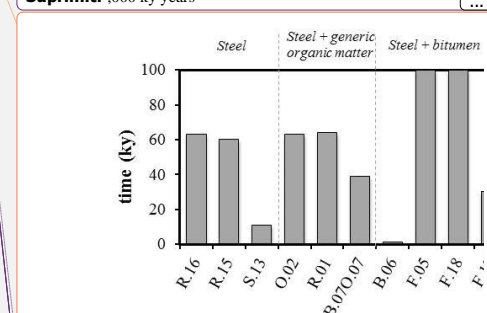
Formatat: anglès (EUA)

Formatat: anglès (EUA)

Formatat [icon]

Suprimir: Figure 6

Suprimir: .000 ky years



Suprimir: [icon]

Formatat: anglès (EUA)

Formatat [icon]

Codi de camp canviat

656 ISA accumulate in solution until precipitation of Ca-acetate and/or Ca-isosaccharinate
 657 occurs. After 5 years, the maximum calculated concentrations of acetate and ISA
 658 achieved are $6 \cdot 10^{-4} \text{M}$ and $5 \times 10^{-3} \text{M}$ respectively. In the long-term, higher concentrations
 659 are calculated. Acetate reaches a maximum of 0.5M. Due to the high solubility of
 660 acetate solids, no acetate is predicted to precipitate and the maximum concentration of
 661 this compound in the system is given by the steady state reached between its generation
 662 and the flow rate at which it is being transported out of the system. An example of the
 663 evolution of the concentration of acetate in solution is shown in [Figure 8](#), or different
 664 waste packages. In contrast, in [Figure 8a](#) the organic matter is completely degraded thus
 665 acetate is no longer generated and it is being transported out of the system while in
 666 [Figure 8b](#), the organic matter generating acetate (bitumen in this case) is never
 667 completely degraded and the concentration of acetate reaches a steady state.

Suprimir: Figure 7 f

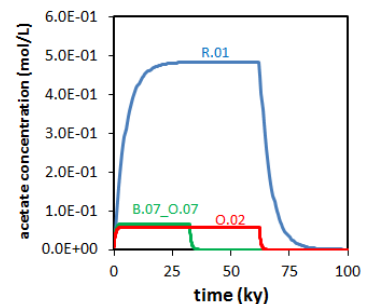
Suprimir: Figure 7

Suprimir: Figure 7b

670
 671
 672 Cellulose is completely degraded before 7 ky after repository closure in three out of the
 673 four waste packages containing cellulose. The concentration of ISA in all cases is
 674 limited to $1.6 \times 10^{-2} \text{ mol/L}$ due to the precipitation of $\text{Ca}(\text{HISA})_2(\text{cr})$ in the presence of
 675 calcium concentrations given by equilibrium with portlandite.

676
 677 In the case of O.12, where granitic groundwater instead of hyperalkaline groundwater is
 678 contacting the waste, the Eh is kept at a less reducing value than in the other cases (-
 679 0.34 V). Due to the carbonate content of the contacting water, the main corrosion
 680 product of steel is in this case siderite.

681
 682 The anoxic corrosion of steel has, as a consequence, the production of $\text{H}_2(\text{g})$ at expenses
 683 of water reduction. $\text{H}_2(\text{g})$ is the most abundant gas generated in the system. According
 684 to the model constraints, hydrogen dissolves and accumulates in solution until the total
 685 gas pressure exceeds the hydrostatic pressure of the repository (6.87 atm). Then H_2
 686 aqueous concentration is kept constant and in equilibrium with $\text{H}_2(\text{g})$. [Figure 9](#) shows
 687 the calculated volume of gas generated in the system. The production of $\text{CO}_2(\text{g})$ is only
 688 relevant in the case of the O.12 waste package (10% vol.) due to the lower pH of the
 689 contacting water.



Suprimir:

Formatat: anglès (EUA)

Formatat: anglès (EUA)

Formatat: anglès (EUA)

Taula formatada

Formatat: anglès (EUA)

Formatat: Tipus de lletra: (Per defecte) Times New Roman, 12 pt, anglès (EUA)

Formatat: anglès (EUA)

Formatat: anglès (EUA)

Suprimir: ,000

Suprimir: years

Suprimir: of the

Suprimir: Figure 8

698
 699 Neither concrete degradation, nor the formation of other corrosion products other than
 700 goethite and magnetite are considered in the calculations. Both processes can, however,
 701 have an important control on the pH or the Eh finally achieved in the repository. [Table 5](#)
 702 shows the Eh/pH field framed by the different redox couples more likely to exert the
 703 redox control in the repository at the different pH values that porewater can reach due to
 704 concrete degradation. In all cases reducing redox potentials are developed. Only in the
 705 case of considering ferrihydrite (HFO) as the oxidation product of magnetite (extreme
 706 case considering the modeling time), mildly reducing potentials could be attained.

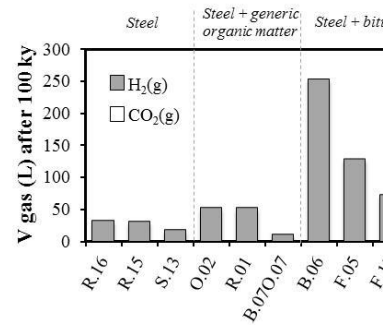
710 4.1. Evolution of the Reducing Capacity (RDC) of the waste package types.

711
 712 The initial RDC in the system is given by steel and the different type of organic matter
 713 considered (generic organic matter, bitumen and cellulose).

714
 715 Steel is considered to corrode mainly to magnetite (except under the conditions of O.12
 716 where siderite is formed) that, due to its Fe(II) content, still presents RDC. The length of
 717 the period during which steel is the main contributor to the RDC ([Figure 10](#)) depends on
 718 the rate of steel corrosion, which is in turn dependent on the reactive surface of the steel,
 719 as well as on the initial amount of steel in a given waste package type.

720
 721 In spite of the potential role that organic matter or bitumen can have in the reductive
 722 capacity of the system, the uncertainties on their degradation kinetics might decrease
 723 their effective role down to insignificant values. For this reason, the RDC of the waste
 724 package types containing organic matter or bitumen besides steel has been calculated
 725 with and without considering the contribution of organic matter or bitumen remaining in
 726 the waste. Therefore, main contributors to the RDC are also in this case steel and
 727 magnetite. As already mentioned, observed differences between the RDC of the
 728 different waste package types depend on the amount of steel and its reactive surface.

729
 730 Cellulose is totally degraded before 7,ky, except in one of the waste packages (F.23),
 731 where the contribution of cellulose to the RDC of the package is relevant in the time
 732 period assessed ([Figure 10](#)).



Suprimit: Figure 8. Gas volume generated after 100,000 ky years in each one of the waste package types.¶

Formatat: anglès (EUA)

Formatat:

Suprimit: Table 5

Suprimit: Table 5. Table 5. Range of redox potential calculated depending on the active couple considered to control the system and the pH marked by the degradation of cementitious materials. A specific calculation is indicated for O.12, with no cementitious materials present. Fe₂O₃: hematite; FeOOH: goethite; Fe₃O₄: magnetite; HFO: ferrihydrite.¶

Formatat: anglès (EUA)

Formatat:

Formatat: anglès (EUA)

Formatat: anglès (EUA)

Formatat:

Formatat: anglès (EUA)

Formatat:

Formatat: anglès (EUA)

Formatat:

Formatat: anglès (EUA)

Formatat:

Formatat: anglès (EUA)

Formatat:

Formatat: anglès (EUA)

Formatat:

Formatat: anglès (EUA)

Suprimit: (Figure 9)

Suprimit: ,000 ky years

Suprimit: (Figure 9)

762

763

764

765

4.2. Evolution of the Reducing Capacity (RDC) of the repository.

767

The evolution of the overall RDC of the different vaults of the SFR repository has been estimated by considering the number of each type of waste packages in each vault.

769

770

Figure 11 shows the temporal evolution of the RDC for the four vaults and for the Silo of the SFR repository. In the early times of evolution, BLA presents the highest RDC of the repository, BMA is the vault most contributing to the RDC of the repository at intermediate and long-term, and 1&2BTF and BLA are the vaults with the lowest RDC values in the long-term, therefore the most susceptible of losing the reducing conditions under the event of an oxidant intrusion). In none of the cases the RDC goes to zero, showing that after 100 ky, under non-disturbing conditions, the system is sufficiently robust as to keep the reducing conditions imposed by the process of steel corrosion.

778

779

Steel corrosion rates available in literature span over more than 4 orders of magnitude depending on the type of material studied, the conditions imposed and the methods used in the steel corrosion rate determination (measurement of the hydrogen evolution, current intensity, and metal loss or gain).

784

785

Data in Smart et al. (2004) have been used to define the Probability Distribution Function (PDF) for steel corrosion rate under alkaline conditions. In the light of the existing corrosion rates, a PDF of the natural logarithm of the rate (in $\mu\text{m}/\text{y}$) with an average of -2.61 and a standard deviation of 0.60 has been determined. Sensitivity calculations have been conducted with the waste package type S.13, and the software MC-PHREEQC (de Vries et al., 2012) which provides a way to conduct Monte-Carlo simulations automatically. The results can be seen in Figure 12 for 4 different times.

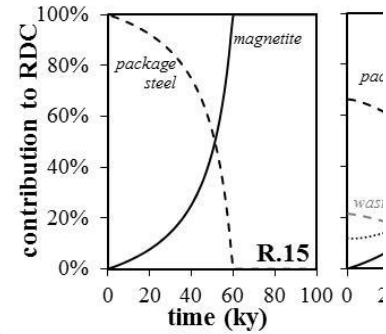
792

The RDC of S.13 waste package type after 100 ky is not very affected by the uncertainty in the corrosion rate, given that steel has been already completely corroded and the remaining RDC is provided by magnetite. For a corrosion rate of 2×10^{-10}

793

794

795



Suprimit: Figure 9. Contribution of magnetite, steel, cellulose and siderite to the calculated RDC (in %) in the waste package types R.15, F.23 and O.12.

Formatat: Tipus de lletra: (Per defecte) Times New Roman, 12 pt

Formatat: anglès (EUA)

Formatat: anglès (EUA)

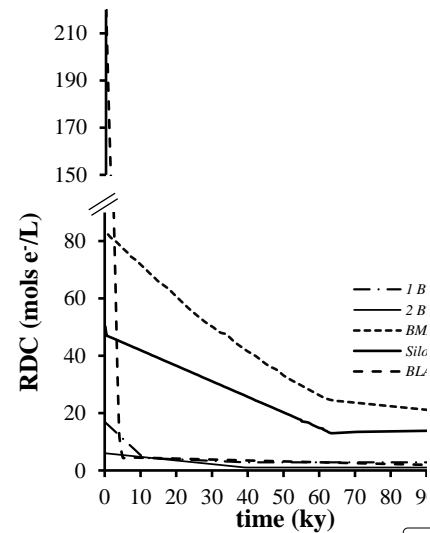
Formatat: anglès (EUA)

Formatat: anglès (EUA)

Suprimit: Figure 10

Formatat: No Marca

Suprimit: e



Formatat: anglès (EUA)

Formatat: anglès (EUA)

Formatat: anglès (EUA)

Formatat: anglès (EUA)

Suprimit: Figure 11

810 mole/m²/s (0.05 μm/y) after 5ky the RDC remaining only relies on magnetite, while
 811 when the rate is 1×10⁻¹⁰ mole/m²/s (0.025 μm/y) steel is still present in the system after
 812 5ky and provides additional RDC to the system. As expected, for short time periods,
 813 higher RDC are obtained for lower corrosion rates.

814

815
 816 The effect of a glacial event in the RDC of a waste package type has been tested with
 817 the S.13 waste package type. As seen in Figure 7, steel contained in S.13 is completely
 818 corroded around 11 ky after the closure of the repository. From this moment onwards,
 819 most of the RDC of the system is provided by magnetite. In SKB (2008) it was
 820 considered that the earliest melt water flow will occur at 60ky after the closure of the
 821 repository. Glacial groundwater (composition in Table 4) has been assumed to flow
 822 through the S.13 from the moment of the glacial event (after 60ky of the deposition of
 823 the wastes) to the end of the period of interest (100 ky), that is for a period of 40 ky.

824

825 The results of the calculation indicate that at the end of the assessment period of interest
 826 (100 ky) the system has not been depleted of its RDC, which is equivalent in this
 827 simulation to say that not all magnetite has been transformed into goethite and,
 828 therefore, the system is still able to buffer an oxidant intrusion (Figure 13). After 40ky
 829 of infiltration of meltwater, the amount of magnetite oxidised into goethite is 95%, and
 830 5% of the magnetite remains unoxidised.

831

832 The amount of magnetite in the system provides enough RDC as to counteract an O₂
 833 intrusion for more than 50 ky. After this period Eh increases.

834

835

836 4.3. Assessment of the behaviour of Se, Tc, Np and Pu

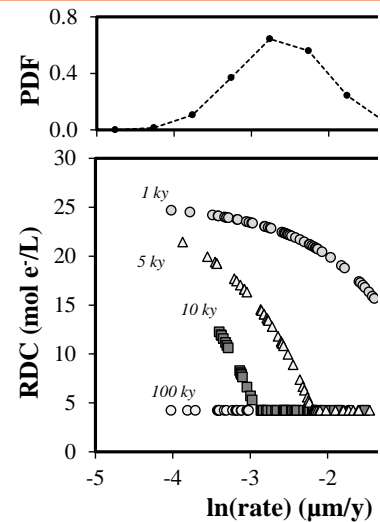
837

838 4.3.1. Selenium

839

840 Se speciation is dominated by Se(-II) species, mainly HSe⁻ in the reducing period of
 841 time. Neither the presence of acetate nor ISA in solution affects the Se aqueous
 842 speciation. The most favoured solid phase to be formed under the conditions of the
 843 assessment is Se(cr), if the concentrations of Se are high enough. Depending on the

Suprimit: aft



Suprimit:
 Figure 11. Variation of the RDC due to changes in steel corrosion rate accordingly to the PDF function calculated for S.13 waste package type at different times. ¶

Formatat: anglès (EUA)

Formatat

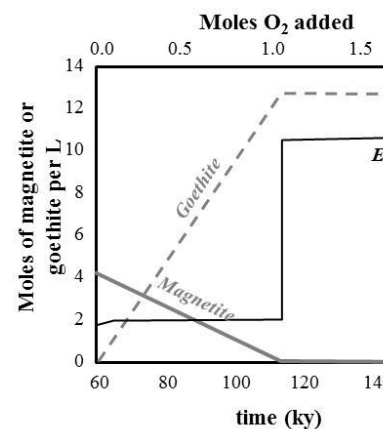
Suprimit: Figure 6

Suprimit: Table 4

Suprimit: ,000 ky years

Suprimit: Figure 12

Suprimit: of a 95%, and a



Suprimit:
 Figure 12. Evolution of the moles amounts of magnetite and goethite in S.13 waste package type and the value of the redox ¶

Formatat: anglès (EUA)

Formatat

Suprimit: Tc,

881 concentration of Fe present in the system, Fe(II) selenides can form, reducing the
 882 mobility of Se. According to the available thermodynamic data, the precipitation of
 883 these phases will require concentrations of Fe in solution higher than the ones calculated
 884 to be present in the system.

885

886 As shown in [Figure 14](#), vaults inventories are lower than calculated solubilities except
 887 for the BLA, where the formation of metallic Se could account for a more effective
 888 retardation mechanism than for the other vaults. Therefore, the most likely retention
 889 mechanism for Se is not expected to be precipitation, but interaction with solid surfaces
 890 of the system.

891

892 4.3.2. Technetium

893

894 As in the case of Se, no influence of ISA or acetate on the chemical behaviour of Tc
 895 under the conditions of interest is expected. Under reducing conditions Tc can
 896 precipitate as $TcO \cdot 1.63H_2O(s)$, while under oxidising conditions Tc is mainly soluble as
 897 $Tc(VII)$, forming the oxyanion pertechnetate (TcO_4^-). Under reducing conditions the
 898 main aqueous species are $TcO(OH)_2(aq)$ and $TcO(OH)_3^-$.

899

900 In the BLA vault, the Tc inventory is below the calculated solubility limit in all cases,
 901 implying that Tc will not be solubility limited in this vault ([Figure 14](#)). In the case of
 902 IBTF, the inventory is either below or very close to the solubility limit ($6.7 \times 10^{-9}M$),
 903 indicating that solubility will neither be an important retardation process for Tc in this
 904 vault.

905

906 Regarding the SILO, BMA and 2BTF vaults, the calculated solubility is below the
 907 inventory only in the case of pH = 10.5, that is when concrete has been degraded to
 908 CSH. This would also point towards other retardation processes, such as sorption on the
 909 surface of cement degradation phases or iron corrosion products, as mainly contributing
 910 to the retention of Tc in the system.

911

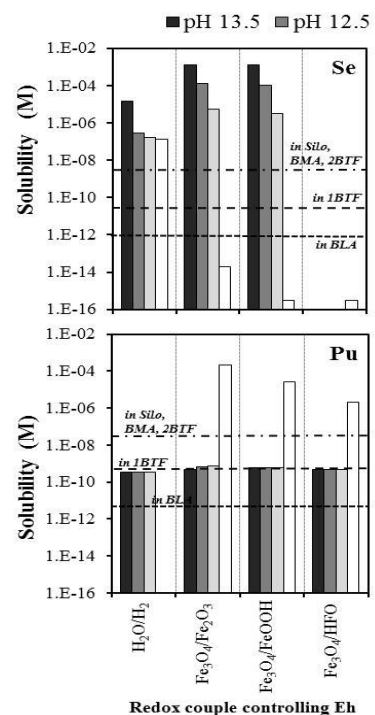
912

913 4.3.3. Neptunium

914

Suprimit: Figure 13,

Suprimit: Figure 13).



Suprimit:
 Figure 13. Comparison between dissolved inventory of Se, Tc, Np and Pu in the different vaults (dashed lines) with the solubility of these radionuclides assuming the formation of the most stable phase under the geochemical conditions expected in the vaults.¶

Formatat: Tipus de lletra: (Per defecte) Times New Roman, 12 pt, Negreta

Formatat: anglès (EUA)

Formatat: anglès (EUA)

Formatat: anglès (EUA)

Formatat: anglès (EUA)

922 The most likely solid phase that can be formed under the conditions of the assessment is
923 the tetravalent $\text{NpO}_2 \cdot 2\text{H}_2\text{O}(\text{am})$ whose precipitation occurs at concentrations above 10^{-9}
924 M in the absence of organic ligands. The effect of acetate on the Np solubility is
925 negligible at the acetate concentrations calculated in the SFR. At pH 12.5 and reducing
926 Eh value, an increase of the concentration of ISA produces the predominance of
927 aqueous complexes of Neptunium with ISA and causes an important increase in the
928 solubility of this solid (see [Figure 15 and Figure 16a](#)). The high concentration of Ca
929 imposed by the equilibrium portlandite, favours the precipitation of calcium
930 isosaccharinate and limits the concentration of ISA available for Np complexation, as
931 shown in [Figure 16a](#). The inventory of Np in 1BTF and in BLA is below the solubility
932 limit of Np under all the conditions of the assessment, what means that the most
933 relevant retention processes in these cases will not be precipitation of secondary phases
934 but sorption onto the surface of the major solid phases present in the system,
935 presumably cement and its degradation products as well as iron oxides ([Figure 14](#)).

936

937 In the case of the SILO, BMA and 2BTF, the inventory of Np is slightly above the
938 calculated solubility of Np, thus setting the control of the Np concentration to values
939 about 10^{-9} moles/L given by the solubility of Np(IV) oxides.

940

941 4.3.4. Plutonium

942

943 Pu(IV) and Pu(III) species dominate the speciation of Pu and the precipitation of
944 $\text{PuO}_2 \cdot 2\text{H}_2\text{O}(\text{am})$ is favoured under the conditions of the assessment. Acetate complexes
945 are only relevant for pH below 9.5 and in the absence of calcium. As in the case of Np,
946 the concentration of Ca in equilibrium with portlandite produces the precipitation of
947 calcium isosaccharinate and limits the concentration of ISA available for the
948 complexation with Pu ([Figure 16.b](#)).

949

950 The inventory of Pu in the wastes is definitively over the calculated solubility limits for
951 the SILO, BMA and 2BTF vaults. If neglecting the effect of organics in the vaults, the
952 maximum concentration of Pu in the SILO, BMA and 2BTF can be limited to values
953 around 10^{-9} M due to the precipitation of Pu(IV) oxides under the conditions of pH and
954 Eh covered by this assessment. Nevertheless, the solubility of Pu in the presence of ISA
955 would be increased to values around 10^{-6} M, thus the concentration of Pu in solution

Suprimir: Figure 14 and Figure 15a

Suprimir: Figure 14 and Figure 15a

Formatat: Tipus de lletra: 14 pt

Formatat: Tipus de lletra: 14 pt

Suprimir: Figure 15a

Suprimir: Figure 15a

Suprimir: Figure 13

Suprimir: Figure 15.

Suprimir: Figure 15.b

963 will be controlled either by the inventory or by sorption processes also in the case of the
964 SILO, BMA and 2BTF vaults (Figure 14).

Suprimit: Figure 13

Suprimit: Figure 13

966

967

968 5. CONCLUSIONS

969

970 The main purpose of the work presented here has been the development of a
971 methodology to assess the evolution of the redox state and the RDC of a complex
972 system containing different redox active materials over long time periods. The case used
973 for the development of the model has been the SFR1 intermediate and low level waste
974 repository of SKB (Sweden).

975

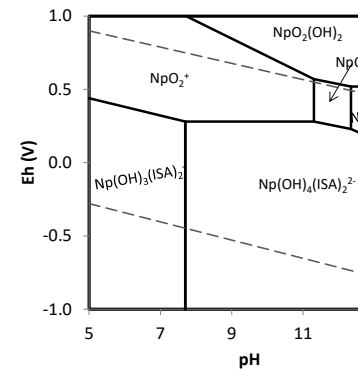
976 The modular configuration applied in the model, by evaluating the individual evolution
977 of the waste packages and combining them to obtain the evolution of the vaults and the
978 complete repository can be transferred to a different geometrical and compositional set-
979 up of the system. This transferability becomes especially relevant in the case of changes
980 in the actual composition of the waste inventory at the time of closure of the repository,
981 or to possible extensions of the SFR1 disposal facility.

982

983 The RDC of the system is mainly provided by steel and organic matter but even under
984 the assumption of redox inertness of bitumen, the assessment shows that the metal
985 content of the waste packages is enough as to provide RDC for the complete time of the
986 assessment (100 ky). Corrosion of steel keeps the system under reducing conditions for
987 long time periods. The role of organic matter is important, especially at the initial stages
988 after repository closure, when microbial activity contributes to a fast oxidant
989 consumption through degradation.

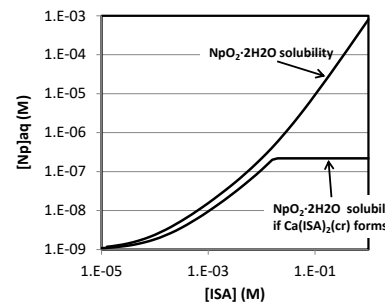
990

991 The redox potential in the vaults is calculated to evolve from oxidising at very short
992 times, due the initial oxygen content, to very reducing at times shorter than 5 years after
993 repository closure. The redox potential imposed by the anoxic corrosion of steel and
994 hydrogen production is on the order of -0.75 V at pH 12.5 in case of assuming that the
995 system responds to the Fe(III)/Magnetite equilibrium. The uncertainty in the response of



Suprimit:
Figure 14. Predominance diagram of aqueous species of neptunium in equilibrium with $\text{NpO}_2 \cdot 2\text{H}_2\text{O}$ (am) in the presence of 0.016 mol/L of ISA.

Formatat: anglès (EUA)



Suprimit:
(a)

Formatat: anglès (EUA)

Formatat: anglès (EUA)

Formatat: anglès (EUA)

Formatat: anglès (EUA)

Formatat: anglès (EUA)

Suprimit: ,000

Suprimit: ears

Suprimit:

1007 the system to a given redox pair combined with the uncertainty regarding the pH
1008 evolution due to concrete degradation brackets the redox potential in values where the
1009 redox sensitive radionuclides are in their most immobile form.

1010

1011 The production of acetate from the degradation of organic matter is not calculated to
1012 affect the mobility of radionuclides, while that of ISA from cellulose degradation can
1013 increase the solubility of plutonium and neptunium up to two logarithmic units.

1014

1015 Most of the gas volume produced is hydrogen, caused by the anoxic corrosion of steel-
1016 related materials, while carbon dioxide only accounts for a maximum of a 10% of the
1017 total volume produced in the waste packages kept at non hyperalkaline values.

1018

1019 Simulations assuming presence of oxic water due to glacial melting, intruding the
1020 system 60 ky after repository closure, indicate that magnetite is progressively oxidised,
1021 forming Fe(III) oxides and that the system is effectively able to buffer a continuous
1022 inflow of oxygen for long periods of time.

1023

1024 6. ACKNOWLEDGEMENTS

1025

1026 This work has been financially supported by SKB (Sweden). I.Puigdomènech, K.
1027 Spahiu, P. Wersin and J. Carlsson are greatly acknowledged for their helpful comments
1028 that contributed to improve the quality of the model. J. Molinero, A. Nardi, L.M de
1029 Vries and P. Trincherro from Amphos 21 have collaborated in the sensitivity analyses of
1030 steel corrosion rate and in the 3D representation.

1031

1032

1033 7. REFERENCES

1034

1035 Almkvist, L., Gordon, A. 2007. Low and intermediate level waste in SFR 1. Reference
1036 waste inventory 2007, SKB Rapport R-07-17. ISSN 1402-3091, 270pp.

1037 Appelo, C. A. J., Postma, D. 2005. Geochemistry, groundwater and pollution. A.A.
1038 Blakema Publishers, the Netherlands, 649 pp.

1039 Avis, J., Suckling, P., Calder, N., Walsh, R. 2012. T2GGM-a coupled gas generation
1040 model for deep geological disposal of radioactive waste. Proceedings, TOUGH

Suprimat: ,000

Suprimat: years

Comentat [CD2]: add reviewers

Suprimat: (

Suprimat:)

- 1045 symposium 2012. Lawrence Berkeley National Laboratory, Berkeley, California,
1046 September 17-19, 2012.
- 1047 Claret, F., Schäfer, T., Bauer, A., Buckau, G. 2003. Generation of humic and fulvic acid
1048 from Callovo-Oxfordian clay under alkaline conditions. *Sci. Total Environ.*, 317, 189-
1049 200.
- 1050 de Vries, L. M., Trinchero, P., and Molinero, J. 2012). MPhreeqc: Extending
1051 geochemical modelling with automatic stochastic simulations. In EGU General
1052 Assembly Conference Abstracts (Vol. 14, p. 6355).
- 1053 Duro, L., Grivé, M., Cera, E., Domènech, C., Bruno, J. 2006. Update of a
1054 thermodynamic database for radionuclides to assist solubility limits calculation for
1055 performance assessment. SKB Technical report TR-06-17, ISSN 1404-0344, 129 pp.
- 1056 Duro, L., Grivé, M., Giffaut, E. 2010. ThermoChimie, the ANDRA thermodynamic
1057 database, in: Buckau, G., Kienzler, B., Duro, L., Grivé, M., Montoya, V. (Eds.), 2nd
1058 annual workshop proceedings of the Collaborative Project “Redox Phenomena
1059 controlling systems” (7th EC FP CP Recosy), KIT Scientific reports 7557, 275-283.
- 1060 Duro, L., Grivé, M., Giffaut, E. 2012. ThermoChimie, the ANDRA Thermodynamic
1061 Database. MRS Proceedings, 1475, imrc11-1475-nw35-o71 doi:10.1557/opl.2012. 637.
- 1062 Elie, M., Faure, P., Michels, R., Landais, P., Griffault, L., Mansuy, L., Martinez, L.
1063 2004. Effects of water-cement solutions on the composition of organic compounds
1064 leached from oxidized Callovo-Oxfordian argillaceous sediment. *Appl. Clay Sci.*, 26,
1065 309-323.
- 1066 Faure, P., Landais, P., Griffault, L. 1999. Behavior of organic matter from Callovo-
1067 Oxfordian shales during low-temperature air oxidation. *Fuel*, 78, 1515-1525.
- 1068 Glaus, M. A., Van Loon, L. R. 2008. Degradation of Cellulose under Alkaline
1069 Conditions: New Insights from a 12 Years Degradation Study. *Environ. Sci. Technol.*,
1070 42, 2906–2911.
- 1071 Glaus, M. A., Van Loon, L. R., Achatz, S., Chodura, A., Fischer, K. 1999. Degradation
1072 of cellulosic materials under the alkaline conditions of a cementitious repository for low
1073 and intermediate level radioactive waste. Part I: Identification of degradation products.
1074 *Anal. Chim. Acta*, 398, 111–122.
- 1075 Grivé, M., Duro, L., Domènech, C., Salas, J. 2011. Redox Evolution of a Cementitious
1076 Geological Disposal Facility. Proceedings of the 13th International High-Level
1077 Radioactive Waste Management Conference (IHLRWMC), 692-700. April 10-14, 2011.
1078 Albuquerque, New Mexico. American Nuclear Society.
- 1079 Holmén, J. G., Stigsson, M. 2001. Modelling of future hydrogeological conditions at
1080 SFR. SKB rapport R-01-02, ISSN 1402-3091, 285 pp.
- 1081 Hummel, W., Berner, U., Curti, E., Pearson, F. J., Thoenen, T. 2002. NAGRA/PSI
1082 Chemical thermodynamic database 01/01, NAGRA Technical Report NTB 02-16, and
1083 Universal Publishers/uPublish.com, Parkland, Florida, USA, 589 pp.
- 1084 Humpreys, P., McGarry, R., Hoffmann, A., Binks, P. 1997. DRINK: a biogeochemical
1085 source term model for low level radioactive waste disposal sites. *FEMS Microbiology*
1086 *Reviews*, 20, 557-571.

Formatat: anglès (EUA)

Suprimit: &

Suprimit: (2012, April

Formatat: anglès (EUA)

Formatat: anglès (EUA)

Formatat: anglès (EUA)

Suprimit: a

Formatat: anglès (EUA)

1090 IAEA 2009. Classification of radioactive waste: safety guide. Vienna, International
1091 Atomic Energy Agency 2009; IAEA Safety Standard series ISSN 1020-525X; no. GSG-
1092 1 STI/PUB/1419, ISBN 978-92-0-109209-0.

1093 Knill, C.J., Kennedy, J.F. 2003. Degradation of cellulose under alkaline conditions.
1094 Carbohydrate Polymers 51, 281-300.

1095 [Lin, Y. H., Lee, K. K., 2001. Verification of anaerobic biofilm model for phenol
1096 degradation with sulphate reduction. Journal of environmental engineering, February
1097 2001, 119-126.](#)

1098 Lindberg, R. D., Runnells, D. D. 1984. Ground Water Redox Reactions: An Analysis of
1099 Equilibrium State Applied to Eh Measurements and Geochemical Modeling, Science
1100 (225), 925-927.

1101 McMahon, P. B., Chapelle, F. H. 2008. Redox processes and water quality of selected
1102 principal aquifer systems. Groundwater 46 (2), 259-271.

1103 Moreno, L., Skagius, K., Södergren, S., Wiborgh, M. 2001. Project Safe Gas related
1104 processes in SFR. SKB rapport R-01-11, ISSN 1402-3091, 130 pp.

1105 Neall, F., 1994. Modelling of the Near-Field Chemistry of the SMA Repository at the
1106 Wellenberg Site: Application of the Extended Cement Degradation Model. Nagra NTB-
1107 94-03.

1108 Parkhurst, D. L., Appelo, C. A. J. 1999. User's guide to PHREEQC - A computer
1109 program for speciation, batch-reaction, one-dimensional transport and inverse
1110 geochemical calculations. Washington D.C., USGS, Water resources investigations
1111 report 99-4259, 312 pp.

1112 Pedersen, K. 2001. Project SAFE. Microbial features, events and processes in the
1113 Swedish final repository for low and intermediate-level radioactive waste. SKB R-01-
1114 05.

1115 Petersson, M., Elert, M. 2001. Characterisation of bitumenised waste in SFR 1. SKB
1116 Rapport R-01-26, ISSN 1402-3091, 62 pp.

1117 Rittmann, B. E., Van Briesen, J. M. 1996. Microbiological processes in reactive
1118 modeling, in: Lichtner, P. C., Steefel, C. I., Oelkers, E. H. (Eds.), Reactive transport in
1119 porous media. Reviews in Mineralogy, 34, 311 – 332.

1120 Roffey, R., Norqvist, A. 1991, Biodegradation of bitumen used for nuclear waste
1121 disposal, Experientia, 47 539-542.

1122 Scott, M. J., Morgan, J. J. 1990. Energetics and conservative properties of redox
1123 systems, in: Melchior, D.C., Basset, R.L. (Eds.) Chemical modelling of aqueous
1124 systems II. ACS Symposium series, 416, 368-378.

1125 Sena, C. 2009. Numerical modelling of radionuclide migration in near-surface systems.
1126 PhD. Thesis. Universidade de Aveiro, Portugal.

1127 SKB, 2008. Safety analysis SFR 1. Long-term safety. SKB rapport R-08-130, ISSN
1128 1402-3091, 373 pp.

1129 Small, J., Humphreys, P., Johnstone, T. J., Plant, R., Randall, M. G., Trivedi, D. P.
1130 2000. Results of an Aqueous Source Term Model for a Radiological Risk Assessment
1131 of the Drigg LLW Site, U.K. MRS Proceedings, 608, 129 doi:10.1557/PROC-608-129.

Suprimit: (

Suprimit:)

Suprimit: ¶

Suprimit: (

Suprimit:)

Suprimit:

Suprimit: and

1139 Small, J. S., Nykyri, M., Helin, M., Hovi, U., Sarlin, T., Itävaara, M. 2008.
 1140 Experimental and modelling investigations of the biogeochemistry of gas production
 1141 from low and intermediate level radioactive waste. *Appl. Geochem.*, 23 (6), 1383-1418.

1142 Smart, N. R., Blackwood, D. J., Marsh, G. P., Naish, C. C., O'Brien, T. M., Rance, A.
 1143 P., Thomas, M. I. 2004. The anaerobic corrosion of carbon and stainless steels in
 1144 simulated cementitious repository environments: A summary review of Nirex research.
 1145 AEAT/ERRA-0313, United Kingdom Nirex Limited.

1146 [SSM 2008. Swedish Radiation Safety Authority Regulatory Code](http://www.stralsakerhetsmyndigheten.se/Global/Publikationer/Forfattning/Engelska/SSMFS-2008-37E.pdf)
 1147 [http://www.stralsakerhetsmyndigheten.se/Global/Publikationer/Forfattning/Engelska/SS](http://www.stralsakerhetsmyndigheten.se/Global/Publikationer/Forfattning/Engelska/SSMFS-2008-37E.pdf)
 1148 [MFS-2008-37E.pdf](http://www.stralsakerhetsmyndigheten.se/Global/Publikationer/Forfattning/Engelska/SSMFS-2008-37E.pdf) SSMFS 2008:37. ISSN 2000-0987.

1149 Stumm, W., Morgan, J.J. 1996. *Aquatic Chemistry*. A Wiley-Interscience Publication.
 1150 John Wiley & Sons, Inc. 1013pp.

1151 Van Loon, L. R., Glaus, M. A., 1994, Experimental and Theoretical Studies on Alkaline
 1152 Degradation of Cellulose and its Impact on the Sorption of Radionuclides. Nagra
 1153 Technical Report NTB 97-04

1154 Van Loon, L. R., Glaus, M. A., Laube, A., Stallone, S. 1999. Degradation of cellulosic
 1155 materials under the alkaline conditions of a cementitious repository for low- and
 1156 intermediate-level radioactive waste II. Degradation kinetics. *J. Environ. Polym.*
 1157 *Degrad.* 7, 41-51.

1158 Wanner, H. 2007, Solubility data in radioactive waste disposal. *Pure Appl. Chem.* 79
 1159 (5), 875-882.

1160 Wersin, P., Johnson, L. H., Schwyn, B., Berner, U., Curti, E. 2003. Redox Conditions in
 1161 the Near Field of a Repository for SF/HLW and ILW in Opalinus Clay. NAGRA
 1162 Technical Report 02-13, 56 pp.

1163 Zobell, C. E., Molecke, M. A. 1978. Survey of microbial degradation of asphalts with
 1164 notes on relationship to nuclear waste management. Sandia Laboratories Technical
 1165 Report. SAND-78-1371. Albuquerque, USA.

1166

Suprimit: .

Suprimit: (

Suprimit:)

Suprimit: (

Suprimit:)